INSULATION PERFORMANCE OF THICKLY COATED CONDUCTOR JOINT AND SUPPORT MODELS FOR GAS/SOLID HYBRID INSULATION SYSTEM WITH SF_6 SUBSTITUTE

H. Goshima[1*], H. Shinkai[1] and M. Yashima[1]
[1]Central Research Institute of Electric Power Industry (CRIEPI),
2-6-1 Nagasaka, Yokosuka, Kanagawa 240-0196, JAPAN
*Email: goshima@criepi.denken.or.jp

Abstract: SF_6 has been identified as a greenhouse gas with a high global warming potential. Therefore, in the long term, it may be important to examine the switchover to next-generation apparatuses using an alternative insulation gas. In the selection of an alternative gas, high-pressure natural gases, such as air, N_2, and CO_2, are promising environmentally friendly candidates. However, some strategies for enhancing insulation performance are necessary for their practical applications to apparatuses. In this study, we investigated the possibility of fabricating a gas-insulated apparatus using a gas/solid hybrid insulation system. Because the hybrid insulation system has a structure whose high-electric-field part is insulated using a solid insulator, there is a possibility that the same degree of compactness as that of the present apparatus can be achieved. However, there are important issues to be resolved before practical applications can be achieved, such as a study on methods of jointing and supporting a thickly coated conductor. In this paper, we describe the proposition of actual models jointing and supporting a thickly coated conductor, and evaluate the insulation performance of these models. The obtained results verified that these joint and support models are applicable to the gas/solid hybrid insulation system.

1 INTRODUCTION

SF_6 has been widely used and has contributed to the downsizing and cost reduction of gas-insulated power apparatuses. However, SF_6 has been identified as a greenhouse gas with a high global warming potential (GWP) [1]. Therefore, recycling guidelines for SF_6 in electric power equipment have been established, and a reduction in the amount of SF_6 released into the atmosphere has progressed [2-4]. In the long term, it is preferable to reduce the amount of SF_6 used. Therefore, regarding the replacement of gas-insulated apparatuses, it may be important to examine the switchover to next-generation apparatuses using an alternative insulation gas. In the selection of an alternative gas, it is considered that high-pressure natural gases, such as air, nitrogen (N_2), and carbon dioxide (CO_2), are promising environmentally friendly candidates [5-8]. However, some strategies for enhancing insulation performance are necessary for their practical applications to apparatuses because the dielectric strengths of these gases are about 1/3 that of SF_6.

In this study, we investigated the possibility of fabricating a gas-insulated apparatus using a gas /solid hybrid insulation system with the combined features of a solid insulator and a dielectric gas [9]. Because the hybrid insulation system has a structure whose high-electric-field part is insulated using a solid insulator, there is a possibility that the same degree of compactness as that of the present apparatus can be achieved despite the application of a natural gas. Therefore, the hybrid insulation system may be useful for alternative equipment that can replace the present compact gas-insulated apparatus. However, there are important issues to be resolved before practical applications can be achieved, such as a study on methods of jointing and supporting a thickly coated conductor.

In this paper, we propose a method of jointing and supporting a thickly coated conductor based on electric field analysis. Moreover, we evaluate the insulation performance of the actual models jointing and supporting a thickly coated conductor.

2 BASIC STRUCTURE OF GAS/SOLID HYBRID INSULATION SYSTEM

Figure 1 shows the basic structure of a gas/solid hybrid insulation system for a single-phase model. The central conductor is covered by a solid insulator (dielectric coating) that we assumed to be epoxy resin or polyethylene at a thickness of about 10mm. For analysing the electric field of the cross-sectional structure, the maximum electric field in the gas can be reduced in the presence of the solid insulator and the field distribution tends to become uniform [10].

In this figure, an insulating spacer is installed, and thickly coated conductors are jointed at the insulating spacer. When the thickly coated conductors are simply jointed to each other, or are connected to the insulating spacer, as shown in Figure 1, a triple junction or an interface of the solid insulator appears as the joint part of the conductors that becomes a weak point for electrical insulation. Therefore, we discuss the

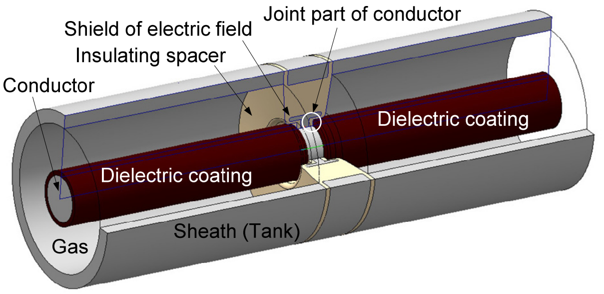

Figure 1: Basic structure of gas/solid hybrid insulation system.

actual structure for jointing and supporting a thickly coated conductor using the results of electric field analysis.

3 ELECTRIC FIELD CALCULATION OF THICKRY COATED CONDUCTOR JOINT AND SUPPORT MODELS

3.1 Calculated models

Figure 2 shows the calculated models jointing and supporting thickly coated conductors. Figure 2(a) shows the "insulating sheath model". The dielectric barrier (insulating sheath) for discharge from the joint part was installed between the coated conductor and the sheath (tank). Moreover, a shield electrode in the insulating spacer was installed at the joint part. Therefore, the electric field of the joint part was shielded.

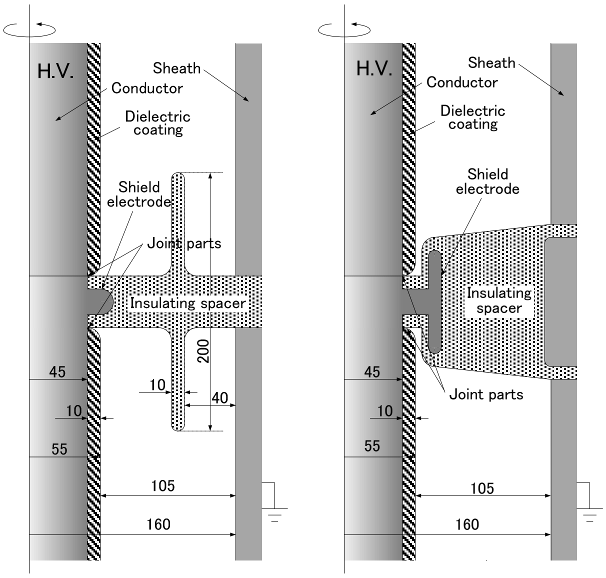

(a) (b)

Figure 2: Thickly coated conductor joint and support models for electric field calculation. (a) Insulating sheath model. (b) Shield electrode model.

Figure 2(b) shows the "shield electrode model". As the longer shield electrode in the insulating spacer was inserted at the joint part, the electric field of the joint part was widely shielded. Furthermore, in the case of the shield electrode model, an opening (gas space) was formed at the contact interface between the coated conductor and the insulating spacer by assuming the elasticity of the coated conductor due to heat.

In these models, basically, the inner diameter of the conductor, the outer diameter of the sheath (tank), and the thickness of the dielectric coating were set to be 90mm, 320mm and 10mm, respectively. The relative permittivity ε_r with the insulating spacer that we assumed to be epoxy resin was set to be 5.0. On the other hand, the relative permittivity ε_r values with the dielectric coatings that we assumed to be polyethylene and epoxy resins were 2.0 and 5.0, respectively. Thus, we calculated the electric field strength of these models using a finite element method and evaluated the maximum electric field in gas.

3.2 Calculated results

Figure 3 shows the calculated results of the electric field distribution for the thickly coated conductor joint and support models (relative permittivity with the dielectric coating: ε_r = 5.0). In this figure, the shade of calculated results indicates the electric field strength, and solid lines are equipotential lines. As mentioned in the previous section, the shield electrode in the insulating spacer was inserted at the joint part, and the electric field of the joint part was suppressed. Although the electric field on the surface (sheath side) of the shield electrode was the highest in the calculated area for both models, a high-electric-field part appeared in the insulating spacer by serving as the joint and support of the coated conductor. Therefore, the maximum electric field strength on the gas side of these models appeared at the surface of the dielectric coating.

Figure 4 shows the electric field strength of the gas side on the surface of the dielectric coating for each model as a function of distance from the joint point for different relative permittivities. It is seen from this figure that the electric field strength near the joint point was suppressed. Moreover, the electric field strength at more than 160mm was nearly equal to the analytical value of the electric field E_d on the surface of the dielectric coating for the coaxial cylinder with infinite length, as shown in Figure 4. That is, E_d=15.6V/mm (at 1kV) for ε_r=2.0, and E_d=16.4V/mm (at 1kV) for ε_r=5.0. It is noted that the analytical value of the electric field for the coaxial cylinder (same size) with the bare conductor was E_d=17.5V/mm. Consequently, the maximum electric field strength on the gas side of these models was lower than that of the simple coaxial cylindrical structure without the dielectric coating (bare conductor) and insulating spacer.

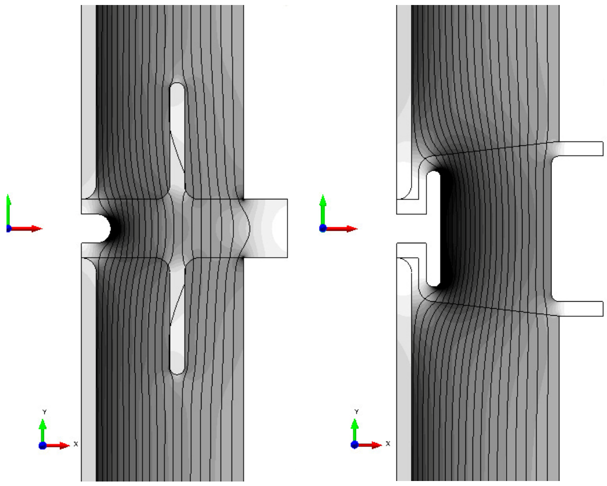

(a) (b)

Figure 3: Calculated results of electric field distribution for thickly coated conductor joint and support models. (a) Insulating sheath model. (b) Shield electrode model.

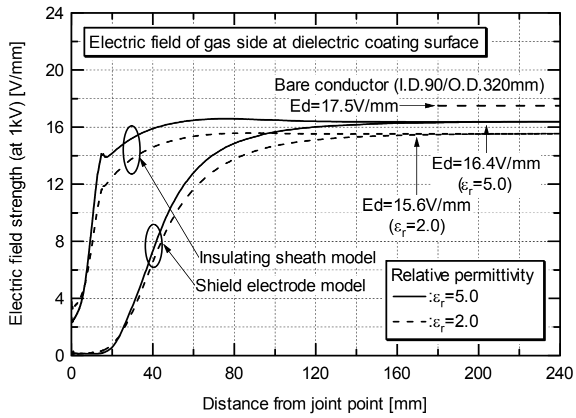

Figure 4: Electric field strength (gas side) at surface of coating conductor as a function of distance from joint point.

4 INSULATION PERFORMANCE OF THICKLY COATED CONDUCTOR JOINT AND SUPPORT MODELS

4.1 Experimental setup

The actual models jointing and supporting the thickly coated conductor for a 300kV-class gas-insulated bus line were tested. Figure 5 shows the structure of the electrode configuration of the shield electrode model, and Figure 6 shows photographs of the installed electrode. Basically, the dimensions of the electrode configuration were the same as those of the calculated models. The diameter of the high voltage central conductor was 90mm, while that of the grounding sheath electrode was 320mm. The effective length of the electrode (flat part) on one side was 200mm. Both electrodes were made of aluminium. The dielectric coating of the conductor was epoxy resin with a filler (silica), and its relative permittivity and thickness were ε_r = 4.5 and 10mm, respectively. The material of the insulating spacer was the same as that of the dielectric coating of the conductor. These models are installed in the test tank (600mm in diameter). The tested natural gas was carbon dioxide (CO_2). The CO_2 gas pressure was set to be 0.5MPa (abs).

A standard negative lightning impulse was applied by a step-up method because the negative lightning impulse was the toughest condition for the electrical insulation of compressed CO_2 gas [5]. It is noted that an interval of more than five minutes is required until the next experiment after the breakdown in order to minimize the effect of the previous breakdown. Thus, the breakdown tests were repeated 15-20 times for each model. The 50% insulation breakdown strength E_{50} (converted from the breakdown voltage) and its variation were estimated by the statistical analysis of the Weibull distribution. The discharge state was checked from the observation window using still cameras.

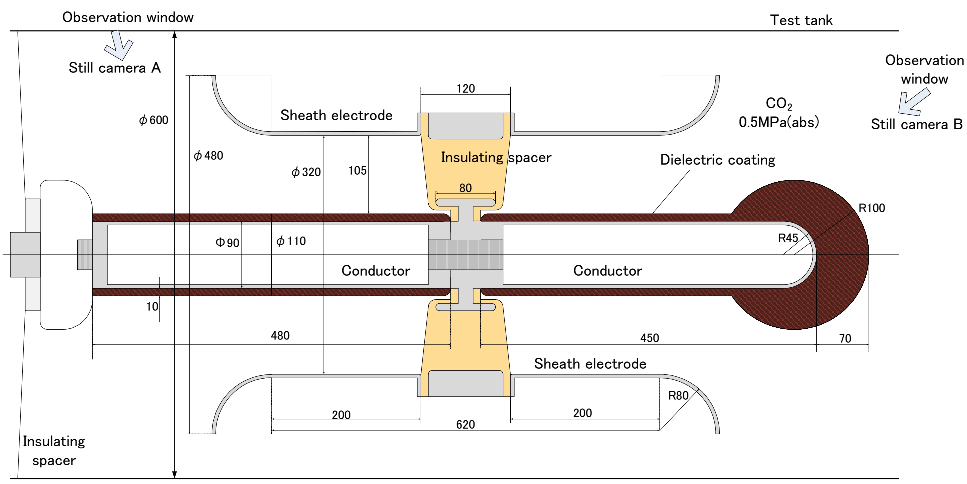

Figure 5: Structure of electrode configuration of shield electrode model.

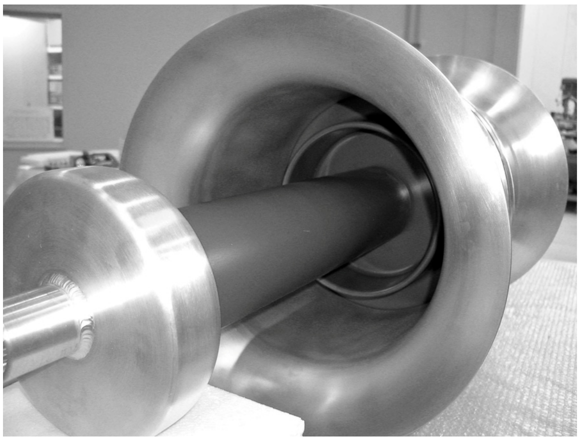

(a)

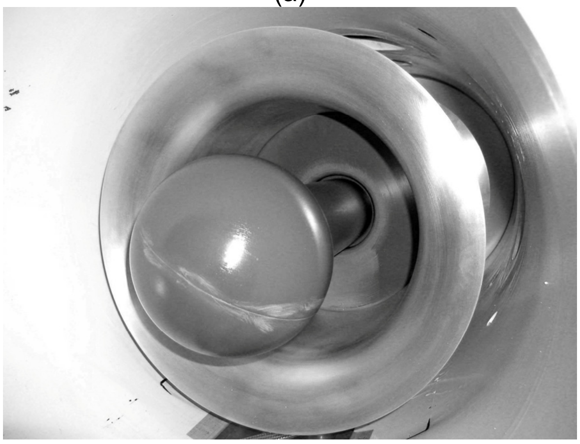

(b)

Figure 6: Overall view of testing model electrodes. (a) Insulating sheath model. (b) Shield electrode model installed in test tank.

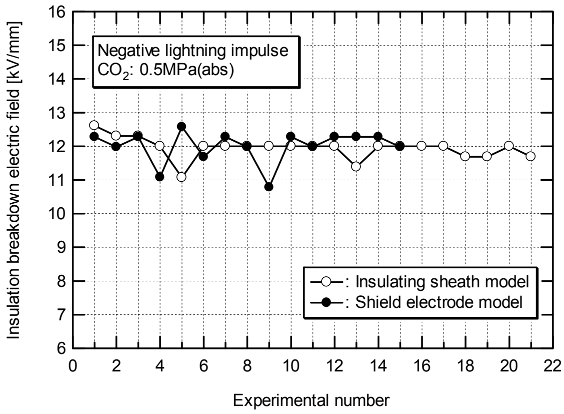

Figure 7: Insulation breakdown electric field as a function of experimental number for different models.

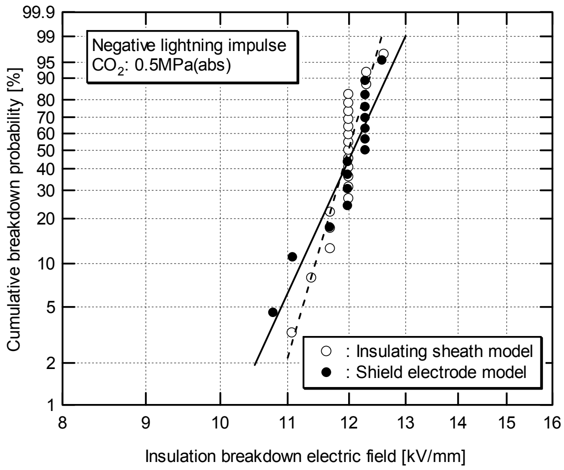

Figure 8: Weibull plots of insulation breakdown electric field for different models.

4.2 Breakdown characteristics

Figure 7 shows the insulation breakdown electric field on the coated conductor surface as a function of experimental number. In this figure, the values of the insulation breakdown electric field for both models are stable for the experimental number. Therefore, it considered that the effect of the previous breakdown in these experiments is negligible.

Figure 8 shows Weibull plots of the insulation breakdown electric field for a negative lightning impulse at a gas pressure of 0.5MPa(abs), and Table 1 shows the various statistics about the insulation breakdown electric field of each model. The 50% insulation breakdown electric fields E_{50} of both models were similar. The variation in insulation breakdown electric field for the shield electrode model was larger than that for the insulating sheath model. However, the values of the standard deviation σ estimated from the shape parameter of the Weibull distribution were less than 5%, the same as those for the breakdown characteristics of compressed CO_2 using the bare electrode [5].

Table 1: Various statistics about insulation breakdown electric field of each model.

Model	Insulating sheath	Shield electrode
Shape parameter m	40.1	25.6
Scale parameter η [kV/mm]	12.1	12.2
E_{50} [kV/mm]	12.0	12.1
Standard deviation σ [%]	3.12	4.83
$E_{50}(1-3\sigma)$ [kV/mm]	10.9	10.3

Figure 9 shows the 50% insulation breakdown electric field E_{50} for a negative lightning impulse as a function of gas pressure. In this figure, the gas pressure dependence of E_{50} for the coaxial cylindrical electrode (70mm in conductor diameter, 150mm in sheath diameter) without the dielectric coating and insulating spacer is shown [5], and the E_{50} values of both models are also plotted. It is noted that the error bars of the markers indicate three standard deviation 3σ. It is seen that the E_{50}

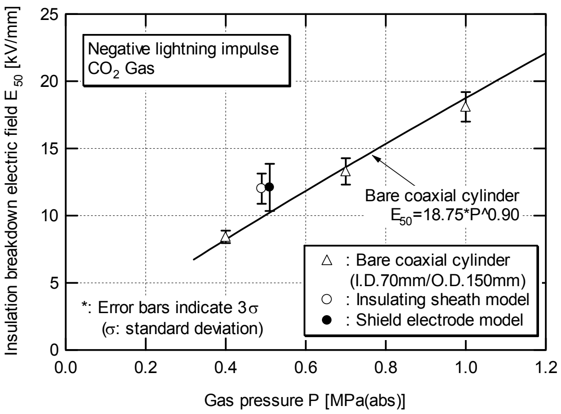

Figure 9: Insulation breakdown electric field E_{50} as a function of gas pressure.

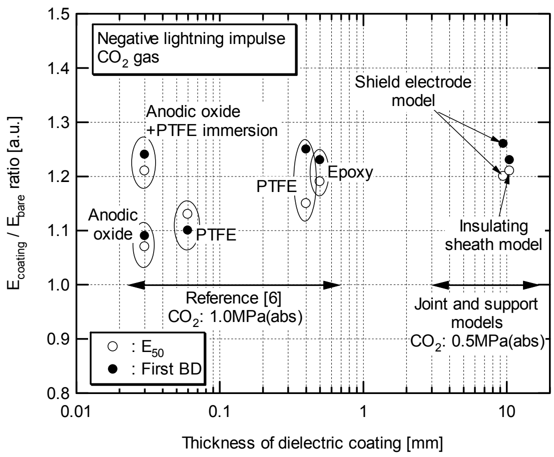

Figure 10: Ratio of insulation breakdown electric field with coated conductor, $E_{coating}$, to that with bare conductor, E_{bare}, as a function of thickness of dielectric coating.

values of both models are approximately 20% higher than that of the coaxial cylindrical electrode at the gas pressure of 0.5MPa (abs).

5 DISCUSSION

5.1 Improvement of insulation breakdown strength

In the previous chapter, it is verified that the insulation performance of the proposed joint and support models was higher than that of the coaxial cylindrical electrode with the bare conductor, despite having the thickly coated joint part. In regard to the conductor coating, the improvement of the insulation performance of the thinly coated conductor was also observed.

Figure 10 shows the ratio of the insulation breakdown electric field with the coated conductor, $E_{coating}$, to that with the bare conductor, E_{bare}, as a function of the thickness of the dielectric coating. In this figure, the plots on the right side are for the proposed joint and support models, and the other plots are cited from [6] where following five types of coating were examined at the CO_2 gas pressure of 1.0MPa (abs): (1) anodic oxide coating on aluminium (thickness: approximately 30μm), (2) anodic oxide coating and immersion of PTFE (thickness: approximately 30μm), (3) fluorine (PFA and PTFA) coating (thickness: 60μm), (4) fluorine (PFA and PTFA) coating (thickness: 400μm), and (5) epoxy resin coating (thickness: 500μm). The value of the first breakdown is important in the application of a dielectric coating to equipment. Therefore, the $E_{coating}/E_{bare}$ ratio for E_{50} and the first breakdown of the experiment are plotted in this figure.

It can be seen from this figure that the improvement of E_{50} for the proposed joint and support models is approximately 20% (25% for the first breakdown), while the maximum level of E_{50} improvement (20%) for the thin dielectric coating without the joint and support parts is the same as that of the proposed joint and support models. Therefore, it is expected that the joint part of the thickly coated conductor with the proposed structure will not become a weak point for electrical insulation, and that the proposed structure will be applicable to the gas/solid hybrid insulation system.

5.2 Discharge path of gas/solid hybrid insulation system

Figure 11 shows examples of the observed discharges for the shield electrode model. This picture was obtained by still camera A, as shown in Figure 5. Therefore, it is impossible to take a discharge path in the main gap including the joint and support parts located on the left side of this picture because of the direction of the observation window. It can be seen from this picture that many discharge paths occurred on the dielectric coating. However, these discharge paths were not the main breakdown path between the high-voltage conductor and the grounding sheath. From the observed discharge paths and the results of breakdown traces after the experiment, a typical discharge path for the gas/solid hybrid insulation system was assumed, as shown in Figure 12. Firstly, a discharge occurred in the gas gap because the surface of the dielectric coating became the part with the maximum electric field. However, after the discharge in gas, puncture breakdown did not occur at the dielectric coating because the thickness of the dielectric coating was large. Therefore, creeping discharges progressed on the dielectric coating. Finally, a breakdown path was formed through the joint part. Note that breakdown traces on the insulating spacer for the shielded electrode model were observed in 4/15 cases, and that most breakdown incidents occurred in the gas part. From this situation, it is expected that the joint part of the thickly coated

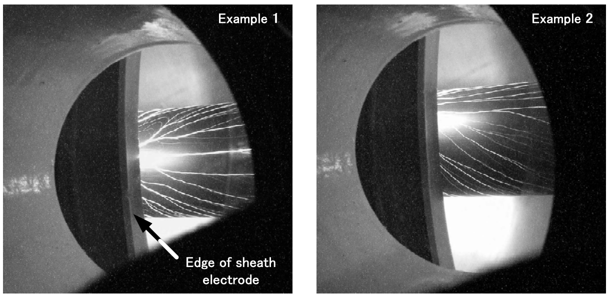

Figure 11: Examples of observed discharges for shield electrode model.

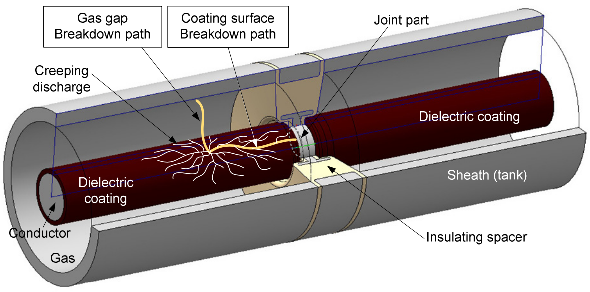

Figure 12: Schematic illustration of discharge path for gas/solid hybrid insulation system.

conductor with the proposed structure will not become a weak point for electrical insulation. Consequently, it is verified that the application of the proposed joint and support structure (particularly the shield electrode model) is a practical method for the gas/solid hybrid insulation system.

6 CONCLUSION

In this paper, we propose a method of jointing and supporting the thickly coated conductor, and evaluate the insulation performance using actual models. The improvement of the insulation performance by applying a thickly coated conductor with the proposed joint and support structure was approximately 20% compared with that in the case of the bare electrode. Consequently, it is verified that the application of the proposed joint and support structure is a practical method for the gas/solid hybrid insulation system.

7 REFERENCES

[1] CIGRE TF01 WG23.10, "SF_6 and the Global Atmosphere", Electra, No.164, 1996.

[2] Electric Technology Research Association Report in Japan, "Standard of SF_6 handling", Vol.54, No.3, 1998. (in Japanese)

[3] CIGRE TF01 WG23.10, "SF_6 Recycling Guide, Re-use of SF6 gas in Electric Power Equipment and Final Disposal", Electra, No.173, 1997.

[4] T. Kawamura, M. Meguro, H. Hama, and T. Yamagiwa, "Industrial Outlook: How to Reduce SF_6 Use and Emission – Various Aggressive Approaches to Realize less SF_6 Environment", Gaseous Dielectrics X, pp.475-484, 2004.

[5] S. Okabe, H. Goshima, A. Tanimura, S. Tsuru, Y. Yaegashi, E. Fujie, and H. Okubo: "Fundamental Insulation Characteristic of High-Pressure CO_2 Gas under Actual Equipment Conditions", IEEE TDEI, Vol.14, No.1, pp.83-90, 2007.

[6] H. Goshima, S. Okabe, T. Ueda, H. Morii, N. Yamachi, K. Takahata, and M. Hikita: "Fundamental Insulation Characteristics of High-Pressure CO_2 Gas for Gas-Insulated Power Equipment –Effect of Coating Conductor on Insulation Performance and Effect of Decomposition Products on Creeping Insulation of Spacer-", IEEE TDEI, Vol.15, No.4, pp.1023-1030, 2008.

[7] K. Juhre, and E. Kynast, "High pressure N_2, N_2/CO_2 and CO_2 gas insulation in comparison to SF_6 in GIS applications," Proc. of 14th ISH, C-01, 2005.

[8] T. Uchii, Y. Hoshina, T. Mori, H. Kawano, T. Nakamoto, and H. Mizoguchi, "Investigations on SF_6-free Gas Circuit Breaker Adopting CO_2 Gas As an Alternative Arc-quenching and Insulating Medium", Gaseous Dielectrics X, pp.205-210, 2004.

[9] H. Goshima, H. Shinkai, T. Kawamoto, M. Yashima, and H. Fujinami: "Estimation of Cross-sectional size of Gas-insulated Apparatus using Hybrid Insulation System with SF_6 Substitute", Gaseous Dielectrics X, pp.253-258, 2004.

[10]M. Yashima, T. Takuma, and T. Kawamoto: "Basic Study on Hybrid-Gas-Insulated Transmission Line (H-GIL)", Proc. of 9th ISH, No.7880, 1995.